American Journal of Geospatial Technology (AJGT)

ISSN: 2833-8006 (ONLINE)

VOLUME 4 ISSUE 1 (2025)

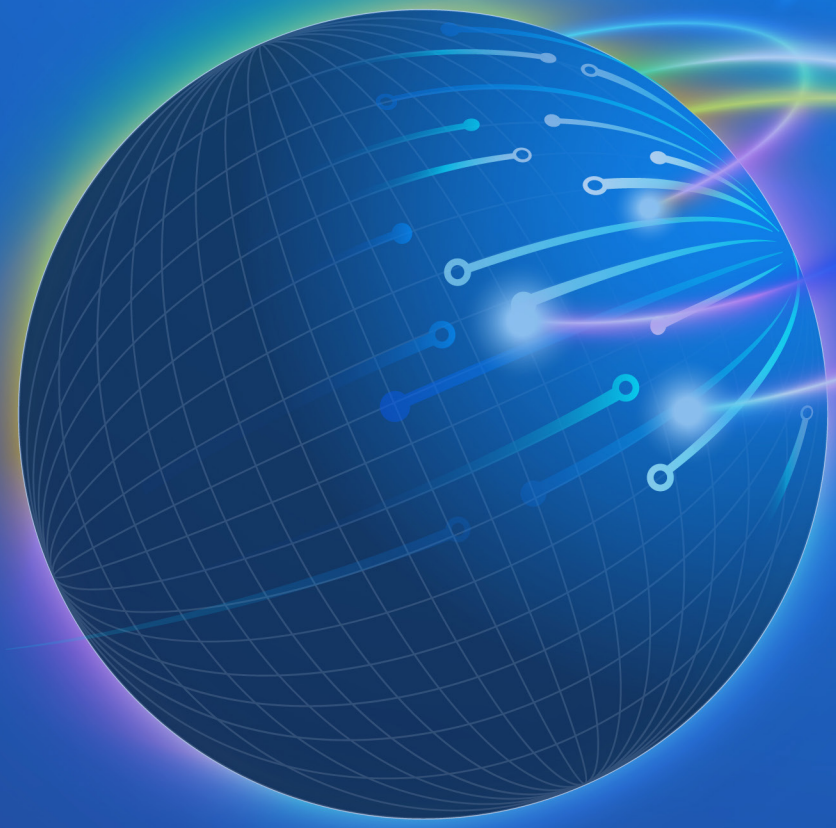

PUBLISHED BY
E-PALLI PUBLISHERS, DELAWARE, USA

American Journal of Geospatial Technology (AJGT)

Volume 4 Issue 1, Year 2025
ISSN: 2833-8006 (Online)
DOI: https://doi.org/10.54536/ajgt.v4i1.4005
https://journals.e-palli.com/home/index.php/ajgt

Mapping and Monitoring Change Detection of High-Altitude Wetland Using Remote Sensing and GIS: A Case Study of Rara Wetland, Nepal

Srijan Thapa[1*], Riya Pokhrel[1]

Article Information

Received: November 14, 2024

Accepted: December 24, 2024

Published: February 07, 2025

Keywords

GIS, High Altitude Wetland (HAW), Rara, Remote Sensing, Spectral Indices

ABSTRACT

High-altitude wetlands (HAW) are essential for the environment as they mitigate climate impacts, facilitate water regulation and groundwater recharge, function as carbon sinks, and promote ecological stability. To protect it from disappearing, it is essential to map and monitor change detection to analyze the extent. However, research on monitoring HAWs remains limited in the world and gets very limited attention. This research uses Geographic Information System (GIS) and remote sensing techniques to analyze the change in Rara wetland extent from 2000 to 2020. We used the Shuttle Radar Topography (SRTM) digital elevation model to generate slope and Topographic Wetness Index (TWI) and Landsat 7 ETM+ images to derive normalized difference Vegetation Index (NDVI), Normalizing Difference Water Index (NDWI) and supervised classification for different years. Over the past two decades, 1.25% of the total area of Rara wetland has been lost at an annual rate of 0.997 hectares. It highlights the urgent necessity for conservation action. This study confirms that GIS and remote sensing effectively delineate, map, and assess wetland dynamics, offering essential insights for future conservation policies and strategies.

INTRODUCTION

Wetland ecosystems are the most endangered environmental resource, which covers approximately 6% of Earth's land (Kerry Turner, 1991). Natural wetlands are shrinking globally, as in the 1970 and 2015, inland and coastal wetlands have decreased by about 35%, (Ramsar Convention on Wetlands, 2018). This rate is three times greater than the rate of forest loss. With this, many critical ecosystem services are lost, such as water and air purification, biodiversity protection, groundwater recharge, food security, and habitats for many endangered species (Gong *et al.*, 2010).

High-altitude wetland (HAW) is defined as "areas of swamp, marsh, meadow, fen, peatland or water located at an altitude above 3000 m, whether natural or artificial, permanent or temporary, with water that is static or flowing, fresh, brackish, or saline"(Chatterjee *et al.*, 2010). These fragile ecosystems are crucial to providing hill communities and large populations in the plain ecological and economic security, regulating water flow, protecting biodiversity, acting as carbon sinks to mitigate climate changes and delivering essential ecosystem services (Trisal & Kumar, 2008); However, HAWs face threats from catchment degradation, changes in hydrological regimes, human-induced pressures, and climate change impacts, and their vital ecosystem services have not been adequately recognized.

In Nepal, four of the nine Ramsar sites are high altitude wetlands: Rara, Phoksundo, Gosaikunda, and Gokyo. The government has taken some initiatives like the National Wetland Policy (2012), the Ramsar wetland site establishment, and the formation of Wetland Management Committees (WMC) at the grassroot level. This shows the efforts have been primarily focused on only policy measures and not on change detection of wetlands. For wetland monitoring, the Geographical information system (GIS) and remote sensing with Landsat data have been used by numerous studies all around the world (Ghobadi *et al.*, 2012; Habiba *et al.*, 2011; Teferi *et al.*, 2010; Wu, 2018). These tools offer the advantage of large-scale, repeated coverage, and comprehensive analysis making them ideal for monitoring spatial-temporal dynamics of wetland distribution.

The major objective of this research is to utilize geographic information systems and remote sensing techniques to map and detect the change in HAW (Rara wetland) and provide valuable insight that will contribute to the conservation efforts of wetland ecosystems and future conservation strategies and policies.

MATERIALS AND METHOD

Study Site

The research area is in Mugu district of western Nepal, which stretches from 81°59'45.48" to 82°19' 14.36" East longitude and 29° 24' 12.44" to 29° 39' 57.25" North latitude cross citation, which covers around 480 km^2. Rara Lake, the focus point in this wetland area, is Nepal's biggest lake. It is located at an altitude of 2990 meters and home to endemic and migratory endangered and vulnerable species. It is roughly 5.1 km long, 3.2 km wide, and 167 m deep home to endemic and migratory endangered and vulnerable species (DNPWC, 2021). This region has an average annual rainfall of around 462mm with an annual yearly temperature is about 11°C with a minimum of 4°C and a maximum of 27°C (RNP, 2019).

[1] International Centre for Integrated Mountain Development (ICIMOD), Kathmandu, Nepal
[*] Corresponding author's e-mail: shrijanthapa01@gmail.com

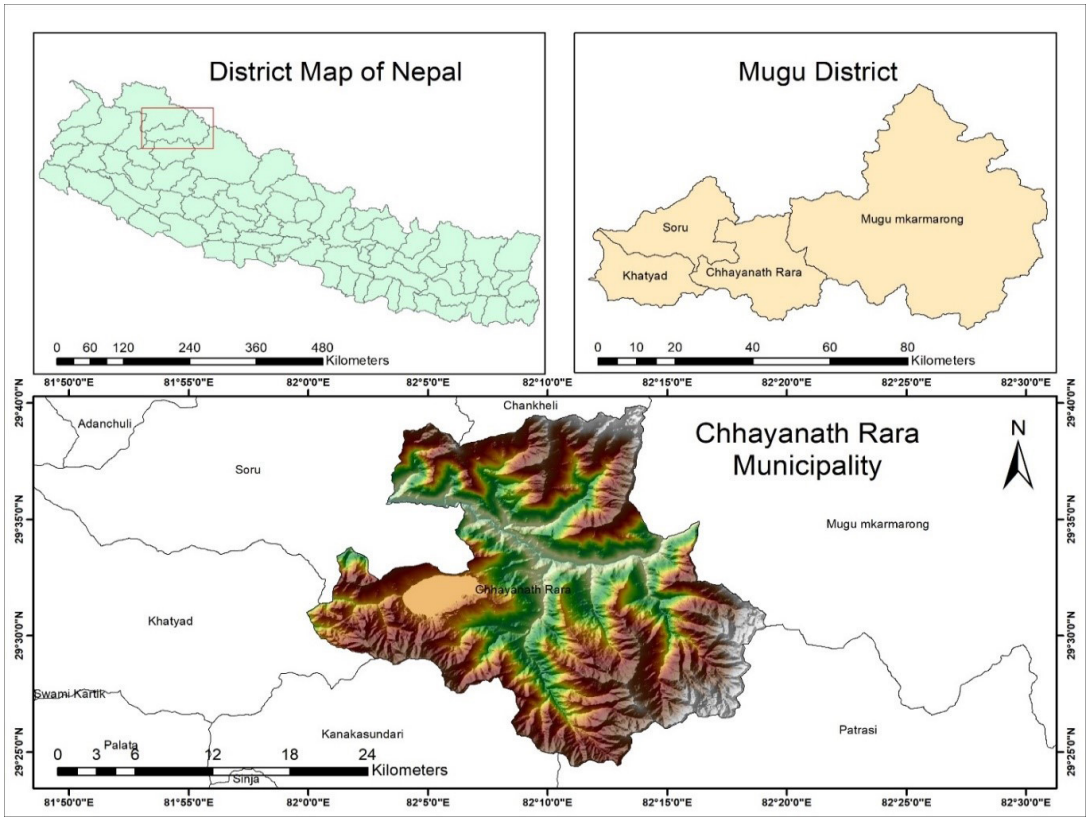

Figure 1: Location map of study area

Imagery and Data

The Landsat ETM+ (Enhanced Thematic Mapper) images and the SRTM digital elevation model of 30m spatial resolution of our research area were downloaded from the United States Geological Survey (USGS) data portal. The Landsat ETM+ images contain eight spectral bands with 30 meters of spatial resolution for bands 1 to 7. The panchromatic Band 8 features a 15-meter resolution. According to (Liu *et al.*, 2005), Landsat images with a 30 meter spatial resolution are precise enough for mapping at a scale of 1:100,000. Table 1 shows the details of satellite images used in this research.

Table 1: Landsat images used in this research

Image	Path/Row	Date of Acquisition
Landsat 7 ETM+	143/040	2000-12-22
Landsat 7 ETM+	143/040	2010-12-18
Landsat 7 ETM+	143/040	2020-12-29

Methodology

Before extracting wetlands, image preprocessing steps were undertaken for all Multi-temporal Landsat images using the ArcGIS software (version 10.8.2) package. These steps included periodic line dropout, radiometric corrections, and atmospheric correction. Furthermore, to derive slope in degree, TWI, NDVI, NDWI, supervised classification, and accuracy assessment were performed using ArcGIS software (Version 10.8.2).

Preprocessing (Periodic Line dropout, Radiometric and Atmospheric Correction)

Periodic line dropouts may occur due to recording issues when one of the detectors in the sensor either provides incorrect data or ceases to function. The Landsat Toolbox's fix Landsat 7 Scanline Errors tool in ArcGIS (version 10.8.2) was employed to address these periodic line dropouts in satellite images. Notably, the Landsat-7 image of 2000 did not contain dropouts, so only correction for periodic line dropouts in the Landsat-7 images of 2010 and 2020 was performed.

Radiometric correction involves deducting the background signal (bias) and dividing by the instrument's gain, thereby converting the raw instrument output (in DN) into radiance. This correction was utilized to convert the digital numbers (DN) of satellite images into both spectral radiance (measured at the sensor) and reflectance.

Following the removal of periodic line dropouts, radiometric correction was applied to multi-temporal Landsat 7 images of 2000, 2010, and 2020. Subsequently, atmospheric correction was performed post-radiometric correction. The aim of atmospheric correction is to rescale the raw radiance data captured by the sensor and convert it into the surface reflectance values to remove atmospheric effects (Hadjimitsis *et al.*, 2010; Tempfli *et al.*, 2009).

Index Based Classification (NDVI, NDWI, TWI, Slope)

These indices have proved to have significant utility in wetland mapping and change analysis across numerous

wetland studies. Incorporating NDWI and NDVI into classification processes resulted in improved outcomes and enhanced distinction of wetland classes, making them widely adopted in wetland delineation efforts(Amani *et al.*, 2021; Ashok *et al.*, 2021; Behera *et al.*, 2012; Dong *et al.*, 2014; Mao *et al.*, 2020; Wu, 2018).

Normalized Difference Vegetation Index

The red band (0.63 µm to 0.69 µm) and near-infrared band (NIR, 0.76 µm to 0.90 µm) are used to calculate the Normalized Difference Vegetation Index (Tucker, 1979). It is the most used index for monitoring change detection of wetland. For analysis of Landsat 7 images, NDVI of respective year images were derived using Band 3 (red) and Band 4 (NIR) (Figure 2).

The formula for calculation is:

NDVI=(NIR-RED)/(NIR+RED) (2.1)

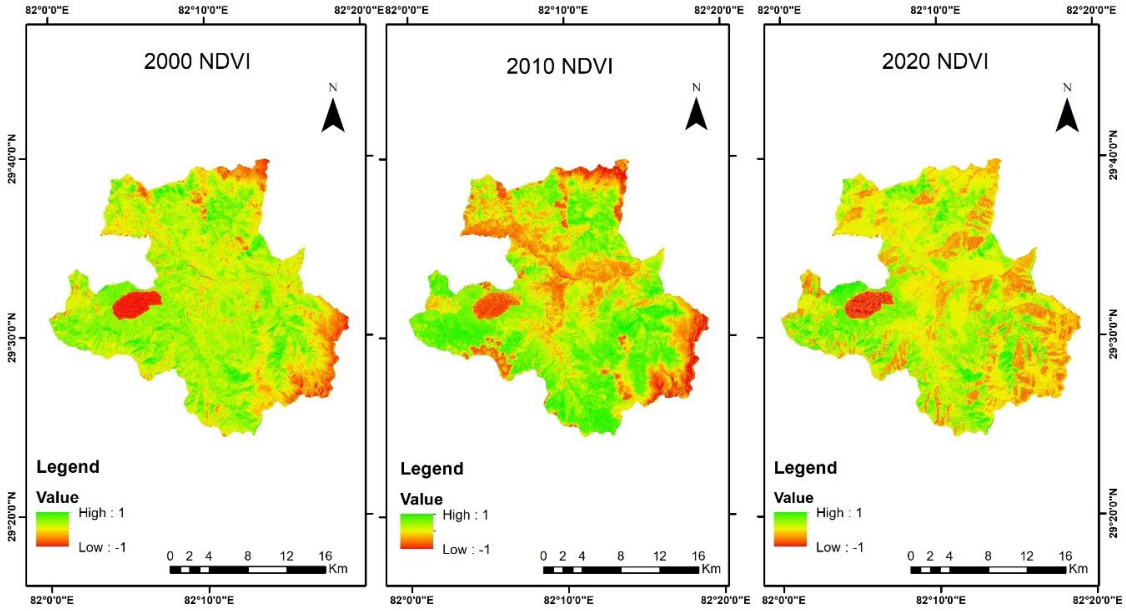

Figure 2: NDVI map for the years of 2000, 2010 and 2020

NDVI values range from -1 to 1, with zero representing bare soil, negative values indicating non-vegetated areas, and positive values signifying vegetation.

Normalized Difference Water Index

Green band (0.52 µm to 0.60 µm) and near infrared (NIR, 0.76 µm to 0.90 µm) bands are used to calculate the NDWI (McFEETERS, 1996). NDWI is employed to identify open water elements and accentuate their visibility in remotely captured digital images, while also filtering out soil and land vegetation features (Figure 3).

The formula for calculating NDWI is:

NDWI=(GREEN-NIR)/(GREEN+NIR) (2.2)

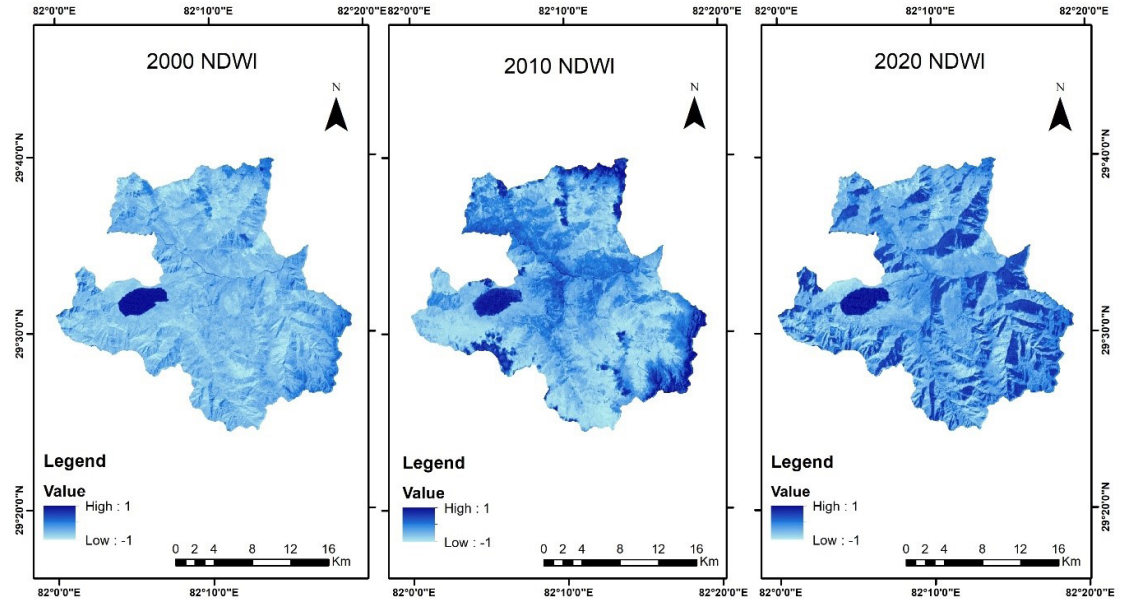

Figure 3: NDWI map for the years of 2000, 2010 and 2020

In Landsat 7 images, band 2 and band 4 denote the green and near-infrared portion of the electromagnetic spectrum respectively. The value of NDWI also ranges from -1 to +1, where negative value indicates vegetation and soil and therefore suppressed, while positive value indicate high vegetation water content thus are enhanced.

Topographic Wetness Index (TWI)

Besides utilizing NDWI and NDVI as indicators of wetlands, topographic position can serve as an additional indicator of wetland presence, constituting a commonly employed approach for detecting and mapping wetlands (Wu, 2018). The TWI is developed by (Beven & Kirkby, 1979) within the runoff model TOP-MODEL. It is computed for each pixel utilizing factors such as drainage area and slope.

Topography Wetness Index (TWI) is expressed as:

$$TWI=\ln(a/\tan(b)) \quad (2.3)$$

Where a is the local up-slope contributing area draining a point per unit contour length and tan b is the local slope.

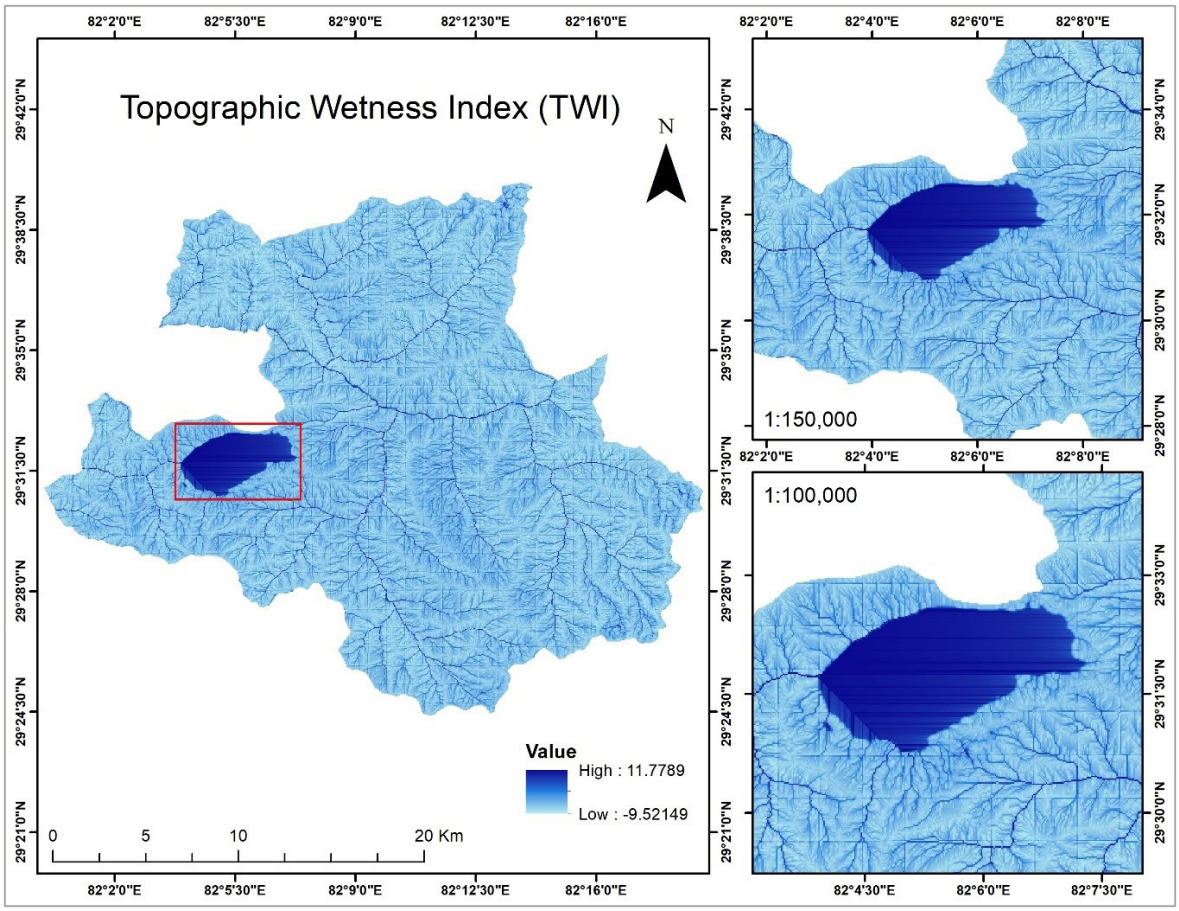

Figure 4: Topographic Wetness Index Map of Study Area

Figure 4 shows the TWI map of the study area where the possible wetland zone is identified as the area with higher potential for water accumulation. TWI assesses a grid cell's tendency to receive and keep water, with higher TWI values indicating greater water accumulation potential in those pixels (Besnard *et al.*, 2013; Sørensen *et al.*, 2006).

Slope

Figure 5 shows the reclassified slope map of the study area with slopes less than 5% was considered the potential wetland area, as many research studies used this threshold in identifying wetland areas (Berhanu *et al.*, 2021; Furlan *et al.*, 2021; Ozesmi & Bauer, 2002; Zhang *et al.*, 2022; Zheng *et al.*, 2017).

Supervised Classification

A supervised classification algorithm typically comprises two phases: the learning or "training" phase, where the algorithm establishes a classification scheme using spectral signatures from "training" sites with known class labels. Generally, as the size of training samples increases, the classification accuracy also rises accordingly, indicating a positive correlation between accuracy and the extent of the training sample region to capture geographical variation (Ma *et al.*, 2017). The second phase is prediction phase, where trained classifier is applied to locations with unknown class membership (Samaniego & Schulz, 2009). Currently, among supervised classification methods for remotely sensed data, the maximum-likelihood classifier stands out as the most widely recognized and utilized.

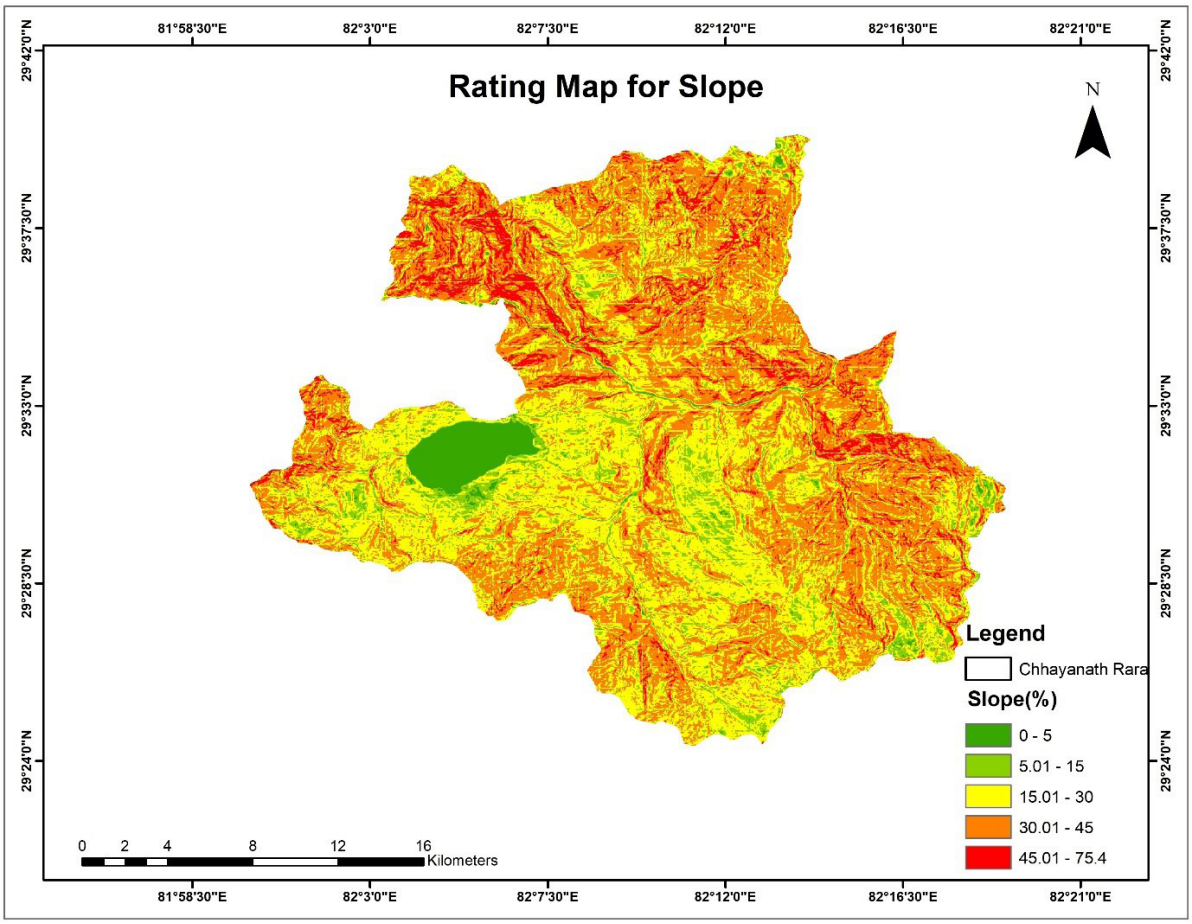

Figure 5: Reclassified Slope Map of Study Area

This is attributed to its statistical robustness, simple and straightforward applicability, and the ease of interpreting the obtained results (ERDAS (Firm), 1997; Lu & Weng, 2007). Because of this advantages and performance maximum likelihood is most commonly used supervised classification technique for wetland mapping (Forgette & Shuey, 2018; Ghobadi *et al.*, 2012; Gosselin *et al.*, 2014; Rebelo *et al.*, 2009).

The maximum likelihood classifier, a parametric supervised classification method, operates on the principle of assigning a pixel to a specific class based on the probability of it belonging to that class. The basic equation supposes that these probabilities are equal for all classes, and that the input bands have normal distributions (ERDAS (Firm), 1997). It uses the training data as a means of estimating means and variances of the classes which are then used to estimate the probability. It considers both the variability of brightness values within each class and average value for classification, unlike minimum distance or parallelepiped (Campbell & Wynne, 2011; Ozesmi & Bauer, 2002). Then the multi-temporal Landsat images of the research area were utilized for land cover classification into five distinct classes: Class 1, designated as Forest; Class 2, representing Agriculture land; Class 3, denoting Grassland; Class 4, designated as Wetland; and Class 5, representing Barren land.

Accuracy Assessment

An accuracy assessment was carried out on classified multi-temporal Landsat imagery, in which entire images were divided into training and testing sets, with 70% allocated for training the maximum likelihood classifier. The selection of training samples involved visually interpreting the imagery and overlaying the final output of index-based classifications, such as NDVI and NDWI. Additionally, derived slope and TWI from the SRTM DEM were used to assist in land cover classification as a complementary data. Subsequently, the remaining 30% of labelled samples were utilized to evaluate the accuracy and reliability of the trained classifier.

To determine the overall accuracy of supervised classification result for year the years 2000, 2010, and 2020, a comprehensive examination employing a confusion matrix is conducted. This analytical tool facilitates a comprehensive comparison of classification outcomes with predefined test site regions of interest, providing key metrics such as user accuracy (UA), overall accuracy (OA), Kappa coefficient (KC), producer accuracy (PA), omission error and commission error.

RESULT AND DISCUSSION

Classification

Land cover maps for the years 2000, 2010, and 2020 were

derived using ArcGIS (version 10.8.2), shown in Figure 6, using the above discussed Methodology. The study area's land cover types were forest, grassland, agriculture land, barren land, and wetland. The study area showed significant changes in its land cover types from 2000 to 2020.

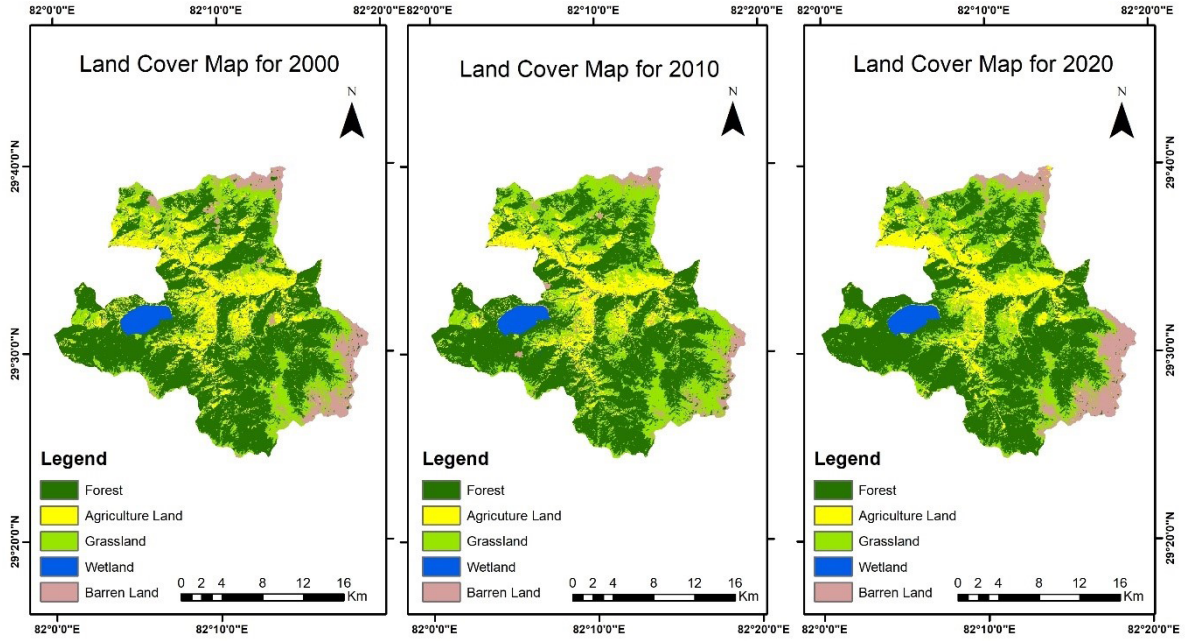

Figure 6: Land cover classifications maps for the year 2000, 2010 and 2020

Figure 7 provides a detailed comparison of the status of these land cover types from 2000 to 2020. 53 % of the study area land was covered by the forest in 2000. This coverage was decline to 51.75% by 2010, but it again increased in 2020 to 52.39%. In 2000, grassland covered 18.11% area of the study area, which was increased to 23.53% by 2010 and again decreased to 21.41% in 2020. The area of agricultural land was decreasing over the years, from 18.02% in 2000 to 15.43 % in 2010 and 13.90 % in 2020. Barren Land also varied, going from 7.64% in 2000 to 6.08% in 2010 before increasing to 9.10% in 2020. The wetland area is also decreasing in a consistent trend with 3.24% coverage in 2000, 3.22% in 2010, and 3.20% in 2020.

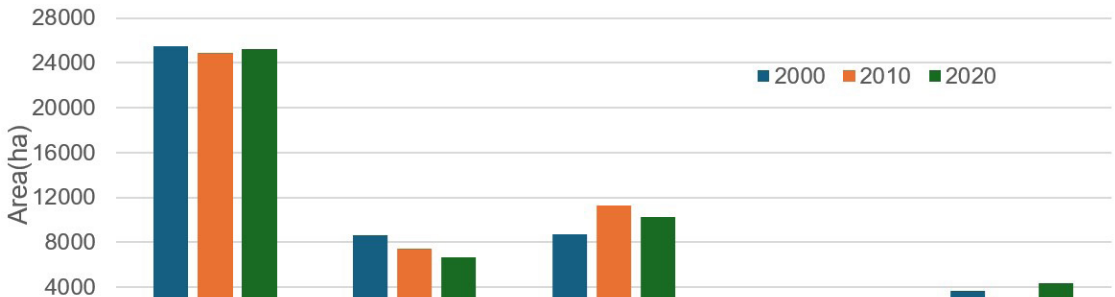

	Forest	Agriculture Land	Grassland	Wetland	Barren Land
2000	25479.14	8663.76	8707.31	1556.24	3671.91
2010	24880.01	7418.43	11312.81	1545.89	2921.22
2020	25187.54	6683.13	10293.65	1536.71	4377.33

Figure 7: Status of Landcover in Study Area

Overall Accuracy Assessment

Additionally, an evaluation of the classification accuracy of the land cover maps derived from Landsat imagery was conducted. Table 2, Table 3, Table 4 displays metrics such as user accuracy (UA), producer accuracy (PA), overall accuracy (OA) and Kappa coefficient (KC) for the classified maps of 2000, 2010, and 2020 respectively. The results indicate that both the overall accuracy and class accuracy (PAs and UAs) exceeded 85% and 80%, respectively, across all maps. Moreover, the Kappa coefficients surpassed 0.81, signifying as almost perfect agreement between the interpreted data and the reference data (McHugh, 2012).

Table 2: Accuracy assessment of land cover classification for 2000

Land Cover	User accuracy	Producer accuracy	Overall Accuracy	Kappa coefficient
Forest	90.31	92.13	87.686	0.831
Agriculture land	80.59	82.59		
Grassland	81.78	81.41		
Wetland	91.68	92.30		
Barren Land	92.01	88.25		

Table 3: Accuracy assessment of land cover classification for 2010

Land Cover	User accuracy	Producer accuracy	Overall Accuracy	Kappa coefficient
Forest	90.10	91.02	88.626	0.845
Agriculture land	81.36	88.72		
Grassland	85.66	86.04		
Wetland	94.80	91.19		
Barren Land	93.40	87.41		

Table 4: Accuracy assessment of land cover classification for 2020

Land Cover	User accuracy	Producer accuracy	Overall Accuracy	Kappa coefficient
Forest	94.73	90.19	90.371	0.867
Agriculture land	85.43	90.15		
Grassland	80.18	91.67		
Wetland	94.62	92.30		
Barren Land	94.45	89.69		

Spatial Distribution and Wetland Change

The analysis indicates a significant reduction in wetland areas within the study region over the past two decades. The wetland area was 1556.24 hectares in 2000, which decreased to 1545.89 hectares in 2010 and further to 1536.71 hectares in 2020 (Figure 8). The overall decrease in wetland area was 1.255% from 2000 to 2020, with an annual degradation rate of 0.977 hectares.

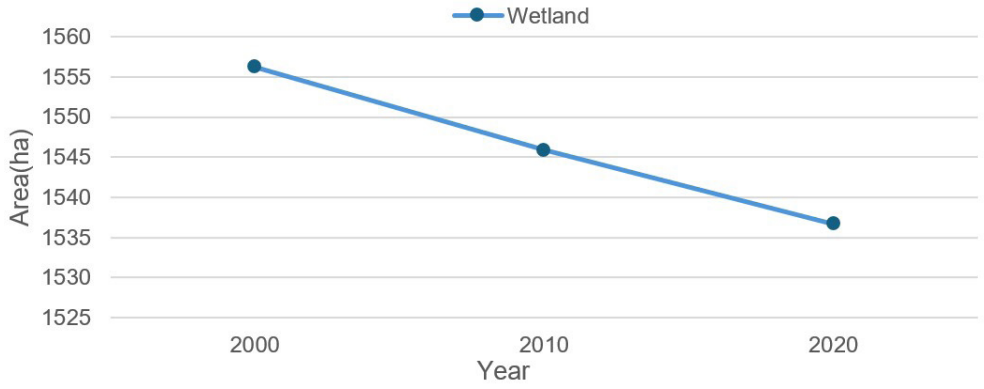

Figure 8: Wetland Degradation graph for the Years 2000, 2010, and 2020

As research done by (Zhang *et al.*, 2022) using Landsat images shows that, due to climate factors such as temperature and evaporation increase, change in precipitation, surface drought, and decreased vegetation coverage, and anthropogenic region, the Maqu wetland area decreased by 23.35% in total, about 261.19 km² from 1999 to 2020. Similarly, the Hokersar wetland has experienced the area degradation from 18.75 km² to 13 km² between 1969 and 2008, marking a loss of 5.75 km² over the last four decades(Romshoo & Rashid, 2014); this decline is primarily due to nutrient and silt load from deforestation, pesticide and fertilizer use, encroachment, unplanned urbanization, and reduced discharge linked to climate change.

The key drivers of wetland degradation and loss are both natural and anthropogenic, which threaten the communities dependent on wetland-based livelihoods. The anthropogenic drivers include infrastructure development, technology use, excessive fertilizer and pesticide use, overexploitation of wetland resources, and agricultural land expansion, whereas natural drivers include climate changes and natural disaster (Bhatta *et al.*, 2018).

The major threats to the high-altitude wetlands are degradation of the catchment area, unplanned and irregular tourism, development activities, and immense grazing pressure (Gujja, 2007). To mitigate the impact and the threats, effective management strategies and wetland management adaptation practices to address the climate changing conditions are crucial to preserve the wetland ecosystem services (Gopal *et al.*, 2010).

Geographic Information System, Remote Sensing and Landsat 7 Images

Geographic information system, when combined with remote sensing utilizing the Landsat 7 ETM+ images, have been effective and accurate tools for mapping wetland areas, monitoring changes, and conducting degradation analysis as demonstrated in various studies (Ghobadi *et al.*, 2012; Rebelo *et al.*, 2009; Teferi *et al.*, 2010). This research utilized Landsat 7 imageries of 30 meters spatial resolution, from which all the GIS layers were created. It has produced excellent results with good accuracy; it still presents challenges in classifying different areas more finely, such as distinguishing between barren and agricultural land or wetlands and other hydric soils. Using a photogrammetry approach (aerial photography) can enhance classification accuracy as it helps in distinguishing different land cover classes, especially if the imageries are captured more frequently during the leaf-off season and on cloud-free days. It reduces errors of omission and commission, particularly those arising from wetlands covered by tree canopies and vegetation present during the leaf-on season (Stubbs *et al.*, 2020).

However, while photogrammetry is suitable for short-term changes and smaller geographic areas, it is not feasible for research like ours, which spans a longer time and covers larger geographic areas, due to the inaccessibility of historical data. In such cases, the fusion of Landsat and SAR data can be utilize which will improves the delineation of field boundaries and radiometric differences, reducing confusion in the classification of natural vegetation with enhancing the classification accuracy (Castañeda & Ducrot, 2009).

This research is carried out using secondary data without site verification and validation. Integrating collected field data with multispectral imagery would help in accurately delineating land cover classes and wetland boundaries. Although this method produced precise and fine results, field data is still a limitation. It is also difficult to carried out field survey in high-altitude wetland due to budget and time required, accessibility, and human constraints. In contrast, satellite remote sensing proves highly beneficial for wetland inventories and monitoring in developing countries with limited funding and sparse.

CONCLUSION

This research has effectively mapped and analysed change detection in the high-altitude Rara wetland using remote sensing and GIS technologies along with multispectral Land 7 ETM+ images. The change in wetland extent has been determined using spectral indices NDVI and NDWI for different years, TWI, slope derived from DEM, and supervised classification for different years. For the past 20 years, 1.25% of the total area of Rara wetland has been lost with a rate of 0.997 hectares annually.

For the years 2000, 2010, and 2020, the overall classification accuracy and Kappa coefficient are above 85% and 0.80 respectively. This accuracy highlights the reliability of remote and GIS for wetland mapping and monitoring. In addition to being cost-effective and efficient, this approach offers a replicable method for analysing and detecting high-altitude wetland changes without carrying out extensive field surveys.

The findings presented in this research have major implications for the conservation of high-altitude wetlands and their ecological functions, such as water and air purification, habitat provision for endangered species, flood protection, biodiversity conservation, preventing shoreline erosion, and water storage. This highlights the urgent need to carry out similar research across all protected high-altitude wetlands and natural wetland areas to monitor changes and undertake restoration efforts.

Our research underscores the urgent necessity to safeguard Rara wetland from further degradation, given the alarming rate of decline. So, decision-makers and concerned authorities must prioritize the implementation of protective strategies to preserve the integrity and functionality of high-altitude wetlands like Rara wetland.

Acknowledgements

The authors thank United States Geological Survey (USGS) for providing the Landsat 7 ETM+ imageries and SRTM DEM. We extend our gratitude to the reviewers for their critical observations and to everyone who contributed to the improvement of this paper.

REFERNCES

Amani, M., Mahdavi, S., Kakooei, M., Ghorbanian, A., Brisco, B., DeLancey, E., Toure, S., & Reyes, E. L. (2021). Wetland Change Analysis in Alberta, Canada Using Four Decades of Landsat Imagery. *IEEE Journal of Selected Topics in Applied Earth Observations and Remote Sensing, 14,* 10314–10335. https://doi.org/10.1109/JSTARS.2021.3110460

Ashok, A., Rani, H. P., & Jayakumar, K. V. (2021). Monitoring of dynamic wetland changes using NDVI and NDWI-based Landsat imagery. *Remote Sensing Applications: Society and Environment, 23,* 100547. https://doi.org/10.1016/j.rsase.2021.100547

Behera, M. D., Chitale, V. S., Shaw, A., Roy, P. S., & Murthy, M. S. R. (2012). Wetland Monitoring, Serving as an Index of Land Use Change-A Study in Samaspur Wetlands, Uttar Pradesh, India. *Journal of the Indian Society of Remote Sensing, 40*(2), 287–297. https://doi.org/10.1007/s12524-011-0139-6

Berhanu, M., Suryabhagavan, K. V., & Korme, T. (2021). Wetland mapping and evaluating the impacts on hydrology, using geospatial techniques: A case of

Geba Watershed, Southwest Ethiopia. *Geology, Ecology, and Landscapes,* 1–18. https://doi.org/10.1080/24749508.2021.1953744

Besnard, A. G., La Jeunesse, I., Pays, O., & Secondi, J. (2013). Topographic wetness index predicts the occurrence of bird species in floodplains. *Diversity and Distributions, 19*(8), Article 8. https://doi.org/10.1111/ddi.12047

Beven, K. J., & Kirkby, M. J. (1979). A physically based, variable contributing area model of basin hydrology / Un modèle à base physique de zone d'appel variable de l'hydrologie du bassin versant. *Hydrological Sciences Bulletin, 24*(1), 43–69. https://doi.org/10.1080/02626667909491834

Bhatta, L. D., Agrawal, N. K., & International Centre for Integrated Mountain Development (Eds.). (2018). *Wetlands in the Himalaya: Securing services for livelihoods.* International Centre for Integrated Mountain Development.

Campbell, J. B., & Wynne, R. H. (2011). *Introduction to remote sensing.* Guilford press.

Castañeda, C., & Ducrot, D. (2009). Land cover mapping of wetland areas in an agricultural landscape using SAR and Landsat imagery. *Journal of Environmental Management, 90*(7), 2270–2277. https://doi.org/10.1016/j.jenvman.2007.06.030

Chatterjee, A., Blom, E., Gujja, B., Jacimovic, R., Beevers, L., O'Keeffe, J., Beland, M., & Biggs, T. (2010). WWF Initiatives to Study the Impact of Climate Change on Himalayan High-altitude Wetlands (HAWs). *Mountain Research and Development, 30*(1), 42–52. https://doi.org/10.1659/MRD-JOURNAL-D-09-00091.1

Department of National Parks and Wildlife Conservation. (DNPWC). (2021). *Rara Lake Ramsar Site Management Plan (2021-2025).* Department of National Parks and Wildlife Conservation.

Dong, Z., Wang, Z., Liu, D., Song, K., Li, L., Jia, M., & Ding, Z. (2014). Mapping Wetland Areas Using Landsat-Derived NDVI and LSWI: A Case Study of West Songnen Plain, Northeast China. *Journal of the Indian Society of Remote Sensing, 42*(3), 569–576. https://doi.org/10.1007/s12524-013-0357-1

ERDAS (Firm). (1997). *ERDAS field guide.* Erdas.

Forgette, T. A., & Shuey, J. A. (2018). A comparison of wetland mapping using SPOT satellite imagery and national wetland inventory data for a watershed in northern Michigan. In C. C. Trettin, M. F. Jurgensen, D. F. Grigal, M. R. Gale, & J. K. Jeglum (Eds.), *Northern forested wetlands* (1st ed., pp. 61–70). Routledge. https://doi.org/10.1201/9780203745380-5

Furlan, L. M., Rosolen, V., Moreira, C. A., Bueno, G. T., & Ferreira, M. E. (2021). The interactive pedological-hydrological processes and environmental sensitivity of a tropical isolated wetland in the Brazilian Cerrado. *SN Applied Sciences, 3*(2), 144. https://doi.org/10.1007/s42452-021-04174-7

Ghobadi, Y., Pradhan, B., Kabiri, K., Pirasteh, S., Shafri, H. Z. M., & Sayyad, G. A. (2012). Use of multi-temporal remote sensing data and GIS for wetland change monitoring and degradation. In *2012 IEEE colloquium on humanities, science and engineering (CHUSER)* (pp. 103–108). IEEE. https://doi.org/10.1109/CHUSER.2012.6504290

Gong, P., Niu, Z., Cheng, X., Zhao, K., Zhou, D., Guo, J., Liang, L., Wang, X., Li, D., Huang, H., Wang, Y., Wang, K., Li, W., Wang, X., Ying, Q., Yang, Z., Ye, Y., Li, Z., Zhuang, D., … Yan, J. (2010). China's wetland change (1990–2000) determined by remote sensing. *Science China Earth Sciences, 53*(7), 1036–1042. https://doi.org/10.1007/s11430-010-4002-3

Gopal, B., Shilpakar, R., & Sharma, E. (2010). Functions and services of wetlands in the Eastern Himalayas: Impacts of climate change.

Gosselin, G., Touzi, R., & Cavayas, F. (2014). Polarimetric Radarsat-2 wetland classification using the Touzi decomposition: Case of the Lac Saint-Pierre Ramsar wetland. *Canadian Journal of Remote Sensing, 39*(6), 491–506. https://doi.org/10.5589/m14-002

Gujja, B. (2007). Conservation of High-Altitude Wetlands: Experiences of the WWF Network. *Mountain Research and Development, 27*(4), 368–371. https://doi.org/10.1659/mrd.mp005

Habiba, U., Haider, F., Ishtiaque, A., Mahmud, M. S., & Masrur, A. (2011). Remote Sensing & GIS Based Spatio-Temporal Change Analysis of Wetland in Dhaka City, Bangladesh. *Journal of Water Resource and Protection, 03*(11), 781–787. https://doi.org/10.4236/jwarp.2011.311088

Hadjimitsis, D. G., Papadavid, G., Agapiou, A., Themistocleous, K., Hadjimitsis, M. G., Retalis, A., Michaelides, S., Chrysoulakis, N., Toulios, L., & Clayton, C. R. I. (2010). Atmospheric correction for satellite remotely sensed data intended for agricultural applications: Impact on vegetation indices. *Natural Hazards and Earth System Sciences, 10*(1), Article 1. https://doi.org/10.5194/nhess-10-89-2010

Kerry Turner. (1991). *Economics and Wetland Management. Ambio, 20*(2), 59–63. JSTOR. http://www.jstor.org/stable/4313777

Liu, J., Liu, M., Tian, H., Zhuang, D., Zhang, Z., Zhang, W., Tang, X., & Deng, X. (2005). Spatial and temporal patterns of China's cropland during 1990–2000: An analysis based on Landsat TM data. *Remote Sensing of Environment, 98*(4), 442–456. https://doi.org/10.1016/j.rse.2005.08.012

Lu, D., & Weng, Q. (2007). A survey of image classification methods and techniques for improving classification performance. *International Journal of Remote Sensing, 28*(5), 823–870. https://doi.org/10.1080/01431160600746456

Ma, L., Li, M., Ma, X., Cheng, L., Du, P., & Liu, Y. (2017). A review of supervised object-based land-cover image classification. *ISPRS Journal of Photogrammetry and Remote Sensing, 130,* 277–293. https://doi.org/10.1016/j.isprsjprs.2017.06.001

Mao, D., Wang, Z., Du, B., Li, L., Tian, Y., Jia, M., Zeng,

Y., Song, K., Jiang, M., & Wang, Y. (2020). National wetland mapping in China: A new product resulting from object-based and hierarchical classification of Landsat 8 OLI images. *ISPRS Journal of Photogrammetry and Remote Sensing, 164,* 11–25. https://doi.org/10.1016/j.isprsjprs.2020.03.020

McFEETERS, S. K. (1996). The use of the Normalized Difference Water Index (NDWI) in the delineation of open water features. *International Journal of Remote Sensing, 17*(7), 1425–1432. https://doi.org/10.1080/01431169608948714

McHugh, M. L. (2012). Interrater reliability: The kappa statistic. *Biochemia Medica, 22*(3), 276–282.

Ozesmi, S. L., & Bauer, M. E. (2002). Satellite remote Sensing of wetlands. *Wetlands Ecology and Management, 10*(5), 381–402. https://doi.org/10.1023/A:1020908432489

Ramsar Convention on Wetlands. (2018). *Global Wetland Outlook: State of the World's Wetlands and their Services to People.* Gland, Switzerland: Ramsar Convention Secretariat.

Rebelo, L.-M., Finlayson, C. M., & Nagabhatla, N. (2009). Remote sensing and GIS for wetland inventory, mapping and change analysis. *Journal of Environmental Management, 90*(7), 2144–2153. https://doi.org/10.1016/j.jenvman.2007.06.027

Rara National Park. (2019). *Rara National Park and its buffer zone management plan 2076/77-2080/81.* Rara National Park Office. https://dnpwc.gov.np/media/publication/Rara_National_Park__its_BZ_ManagementPlan_Printed_version.pdf

Romshoo, S. A., & Rashid, I. (2014). Assessing the impacts of changing land cover and climate on Hokersar wetland in Indian Himalayas. *Arabian Journal of Geosciences, 7*(1), 143–160. https://doi.org/10.1007/s12517-012-0761-9

Samaniego, L., & Schulz, K. (2009). Supervised Classification of Agricultural Land Cover Using a Modified k-NN Technique (MNN) and Landsat Remote Sensing Imagery. *Remote Sensing, 1*(4), 875–895. https://doi.org/10.3390/rs1040875

Sørensen, R., Zinko, U., & Seibert, J. (2006). On the calculation of the topographic wetness index: Evaluation of different methods based on field observations. *Hydrology and Earth System Sciences, 10*(1), 101–112. https://doi.org/10.5194/hess-10-101-2006

Stubbs, Q., Yeo, I.-Y., Lang, M., Townshend, J., Sun, L., Prestegaard, K., & Jantz, C. (2020). Assessment of Wetland Change on the Delmarva Peninsula from 1984 to 2010. *Journal of Coastal Research, 36*(3), 575. https://doi.org/10.2112/JCOASTRES-D-16-00038.1

Teferi, E., Uhlenbrook, S., Bewket, W., Wenninger, J., & Simane, B. (2010). The use of remote sensing to quantify wetland loss in the Choke Mountain range, Upper Blue Nile basin, Ethiopia. *Hydrology and Earth System Sciences, 14*(12), 2415–2428. https://doi.org/10.5194/hess-14-2415-2010

Tempfli, K., Huurneman, G. C., Bakker, W., Janssen, L. L. F., Feringa, W. F., Gieske, A., Grabmaier, K. A., Hecker, C., Horn, J., Kerle, N., Meer, F. D., Parodi, G., Pohl, C., Reeves, C. V., Ruitenbeek, F. J. A., Schetselaar, E., Weir, M., Westinga, E., & Woldai, T. (2009). *Principles of remote sensing: An introductory textbook* (pp. 56–85).

Trisal, C. L., & Kumar, R. (2008). *Integration of High Altitude Wetlands into River Basin Management in the Hindu Kush Himalayas: Capacity Buildings Needs Assessment for Policy and Technical Support.* Wetlands International - South Asia, New Delhi, India. https://lib.icimod.org/record/8445/files/8445-HAwetland.pdf

Wu, Q. (2018). GIS and Remote Sensing Applications in Wetland Mapping and Monitoring. In *Comprehensive Geographic Information Systems* (pp. 140–157). Elsevier. https://doi.org/10.1016/B978-0-12-409548-9.10460-9

Zhang, B., Niu, Z., Zhang, D., & Huo, X. (2022). Dynamic Changes and Driving Forces of Alpine Wetlands on the Qinghai–Tibetan Plateau Based on Long-Term Time Series Satellite Data: A Case Study in the Gansu Maqu Wetlands. *Remote Sensing, 14*(17), 4147. https://doi.org/10.3390/rs14174147

Zheng, Y., Niu, Z., Gong, P., Li, M., Hu, L., Wang, L., Yang, Y., Gu, H., Mu, J., Dou, G., Xue, H., Wang, L., Li, H., Dou, G., & Dang, Z. (2017). A method for alpine wetland delineation and features of border: Zoigê Plateau, China. *Chinese Geographical Science, 27*(5), 784–799. https://doi.org/10.1007/s11769-017-0897-3